

# Using satellite time-series data sets to analyze fire disturbance and forest recovery across Canada

Scott J. Goetz\*, Gregory J. Fiske, Andrew G. Bunn

*Woods Hole Research Center 149 Woods Hole Road, Quissett, Massachusetts 02540, United States*

Received 10 May 2005; received in revised form 4 January 2006; accepted 8 January 2006

## Abstract

The boreal forest biome is one of the largest on Earth, covering more than 14% of the total land surface. Fire disturbance plays a dominant role in boreal ecosystems, altering forest succession, biogeochemical cycling, and carbon sequestration. We used two time-series data sets of Advanced Very High Resolution Radiometer (AVHRR) Normalized Differenced Vegetation Index (NDVI) imagery for North America to analyze vegetation recovery after fire. The Canadian Forest Service Large Fire Database was used to identify the location of fires and calculate scaled NDVI statistics from the Pathfinder AVHRR Land (PAL) and the Global Inventory Modeling and Mapping Studies (GIMMS) AVHRR data sets. Unburned areas were also identified, based on interannual variability metrics, in order to reduce the effects of factors other than fire on the temporal behavior of scaled NDVI. Burned and unburned areas were stratified by ecoregion to ensure the presence of comparable land cover types and account for influences of local environmental variability. Temporal anomalies in NDVI for burned and unburned areas show the impacts of fire and the recovery of the forest to pre-burn levels, and indicate changes in variability that might be associated with vegetation compositional changes consistent with early successional species. The rate of recovery varied in the three episodic fire years on which we focused our analysis (1981, 1989, and 1995), but were consistently shorter than previous studies that emphasized the most impacted areas within fires. Temporal variability in the time series, represented by the difference of burned and unburned area anomalies, increased beyond the observed post-fire recovery period. This indicates residual effects of fire disturbance over the regrowth period, perhaps associated with early successional vegetation and increased susceptibility to drought. Distinct differences were noted between the PAL and GIMMS data sets, with evidence for systematic data processing artifacts remaining in the PAL time series.

© 2006 Elsevier Inc. All rights reserved.

*Keywords:* Fire; AVHRR; FPAR; Boreal forest; Canada; Disturbance; Carbon; Time series

## 1. Introduction

The high latitudes of North America have experienced a 1.5 to 2.0°C warming over the past 30 years (Easterling et al., 2000; Folland et al., 2001) and general circulation models predict substantial warming and drying in the coming decades (Cubasch et al., 2001; Walsh et al., 2002). There is a considerable body of research as to how warming has and will influence the forests and vegetation of the region, and what the implications of warming in high latitudes are for global-scale carbon dynamics.

One of the major issues in understanding how climate change will influence carbon storage in high-latitude ecosystems in the northern hemisphere is accounting for the role of disturbance (Harden et al., 2000; Kasischke & Stock, 2000; Kurz & Apps 1999). In the North American boreal region annual area burned has more than doubled from an average of 14,000 km<sup>2</sup> per year during the 1960s to 31,000 km<sup>2</sup> per year during the 1990s, perhaps as a response to recent warming and drying (Stocks et al., 2000). The increasing frequency and intensity of fire disturbance produces feedbacks on climate through changes in albedo, forest succession, and carbon sequestration by regrowth (Baldocchi et al., 2001; Bonan et al., 1995; McGuire et al., 2001). Energy balance changes after fire when forest cover is reduced and more of the surface substrate is exposed, particularly in intensively burned areas in which the

\* Corresponding author. Tel.: +1 508 540 9900; fax: +1 508 540 9700.  
E-mail address: [sgoetz@whrc.org](mailto:sgoetz@whrc.org) (S.J. Goetz).

organic soil layer is consumed (Baldocchi et al., 2001; Liu et al., 2005). Regeneration gradually decreases albedo as tree canopies establish and, typically, succeed from deciduous broadleaf to evergreen conifer species (Johnstone et al., 2004; Zimov et al., 1999). Net ecosystem carbon exchange, or net ecosystem production, might be affected in less predictable ways, e.g., the balance of respiration terms may completely offset photosynthetic gains in the initial years following disturbance (Houghton, 2003). Boreal areas produce a net CO<sub>2</sub> source to the atmosphere during and shortly after burning that becomes a net sink over following years as regrowth occurs (Amiro et al., 2003; Liu et al., 2005). They typically advance to near equilibrium (small, or no net exchange of carbon) or become moderate net sinks depending on vegetation type, interannual climate variability, and growing season length (Griffis et al., 2003).

Evidence from inverse (tracer transport) models suggest substantial interannual variability in carbon exchange and, for example, strongly enhanced uptake of carbon over North America in the El Niño Southern Oscillation of 1992–1993 relative to 1989–1990, which was not an El Niño year (Bousquet et al., 2000). Other major perturbations include the 1991 Mount Pinatubo eruption which appears, based on model simulations using 64-km<sup>2</sup> AVHRR data sets, to have reduced net primary production (NPP) in boreal regions (Angert et al., 2005; Lucht et al., 2002). In addition to these interannual variations, there is increasing evidence that climate warming is responsible for a trend toward earlier “greening” and increased growing season length in boreal forests (Keeling et al., 1996; Myneni et al., 1997; Slayback et al., 2003), which appeared to result in increased carbon uptake (Chen et al., 2003; Goulden et al., 1998; Nemani et al., 2003; Randerson et al., 1999). Recent evidence suggests that boreal forest greening has abated (Goetz et al., 2005), perhaps due to drought (Angert et al., 2005), although tundra areas continue to respond to climatic warming (Bunn et al., 2005). The results from these analyses have not, for the most part, focused specifically or sufficiently on the role of fire disturbance, which is prevalent in the boreal forest biome, although at least three papers have explored this topic in some depth (Amiro et al., 2000; Hicke et al., 2003; Kasischke & French, 1997).

Kasischke and French (1997) analyzed 14 test sites in the boreal forest of interior Alaska using the AVHRR satellite record and found that patterns of regrowth, as indicated by the NDVI, were defined by the pre-fire vegetation composition, the timing of the fire during the season, and by other landscape factors such as the overall size of the area burned. They note that important information can be derived from these synoptic data sets, but also review some of the limitations of the AVHRR satellite record for studying fire dynamics, including insufficient ability to resolve finer-scale forest patches that follow complex patterns of physiography and soil properties. Amiro et al. (2000) assessed forest carbon budgets following fire using modeled NPP derived from AVHRR leaf area index and land cover type classifications across Canada. They used a single season of these data sets to compare many different years of fire disturbance, effectively yielding snapshots of vegetation

regrowth constrained by the number of burn scar samples in the study area and their associated time since burning. They found NPP increases nearly linearly following fire, through at least the 15-year observation period (1980–1994), and suggest that analyzing growth patterns and responses following fire disturbance would benefit from a longer time series of data. Hicke et al. (2003) then utilized a 17-year time series of AVHRR NDVI data, focusing on 61 large fires in the boreal region of North America. They were able to quantify post-fire NPP recovery relative to pre-fire levels using monthly values of NPP estimated by a carbon model driven with temperature, soil moisture, and scaled conversion factors associated with vegetation light use efficiency. In addition to quantifying vegetation return times, they conclude that fire in the boreal forest can lead to a greater C fluxes to the atmosphere than previously thought.

These studies indicate the need for better estimates of the seasonal and interannual variations that result from fire disturbance, and the associated carbon dynamics of regrowth relative to pre-burn vegetation or comparable unburned areas. Our objective in this paper was to better understand the interannual variability in satellite observations of the Canadian boreal forest in relation to fire disturbance and forest recovery using the AVHRR record (Brown et al., 2004) and the large fire database of Canada (Stocks et al., 2000). First, we sought to compare three of the high (episodic) fire years in the time series to areas of similar extents of unburned land. Second, we sought to capture the magnitude of change in the vegetation density and related properties of the boreal forest, before and following fire disturbance, and to track those changes through the period of record. Third, we sought to determine whether two independently derived time-series data sets of the AVHRR-GAC, the Pathfinder AVHRR Land data set and the Global Inventory Modeling and Mapping Studies Group data set, were qualitatively and quantitatively different in terms of assessing fire across boreal North America.

## 2. Study area

The study area we examined encompassed the entire Canadian boreal forest. One of the largest ecosystems on Earth, it stretches from Alaska to the Canadian Maritime provinces and covers more than five million km<sup>2</sup>. Approximately 20% of the Canadian boreal forest is comprised of wetland or waterways, and the flora is dominated by needle-leaf evergreen species that have adapted to long, cold winters. The burned areas we analyzed for this region crossed 66 unique ecoregions, ranging in diversity from the maritime barrens in Newfoundland to the Klondike Plateau along the Alaskan border. We use the term “ecoregions” as areas of the landscape with a particular set of species and relatively uniform climate (e.g., Bailey, 1998). The Canadian boreal forest was the focus of the Boreal Ecosystem Atmosphere Study (Hall, 1999) and is now a key element of the North American Carbon Program (NACP), a large inter-agency, interdisciplinary research program designed to address various aspects of the carbon cycle.

### 3. Methods

#### 3.1. Data sets

##### 3.1.1. AVHRR time series

Two vegetation index data sets were used in this study; one from the Global Inventory Modeling and Mapping Studies Group (GIMMS version G) (Brown et al., 2004, Pinzon et al., 2004; Tucker et al., 2005) and the other was the Pathfinder AVHRR Land (PAL) data set described by James and Kalluri (1994). Both the GIMMS and PAL data sets were derived from the AVHRR meteorological sensors and are distributed as multi-day NDVI maximum-value composites with a 64 km<sup>2</sup> spatial resolution (Table 1). The GIMMS NDVI data are composited biweekly, with the first 15 days of the month compiled in one file and the remaining days of the same month in another. The PAL NDVI data are binned into “quasi 10-day” composites, that is, the first 10 days of each month are composited in one file, the next 10 days in a second, and the remaining days of the month (8–11) in a third (James & Kalluri, 1994).

A comparison of the GIMMS, Global Vegetation Index (GVI), and the PAL data sets has been conducted by Brown and colleagues (unpublished data). Although each data set originates from the same AVHRR archive, derived from seven different instruments onboard the NOAA meteorological satellites, different processing techniques have improved upon previous versions of the derived products. The enhanced GIMMS data set allows large-scale and long-term vegetation change research, extending the shorter observational period of data provided by more modern satellite platforms (MODIS, SPOT-VGT). The various processing techniques address radiometric calibration, geographic navigation, satellite orbital drift and other environmentally driven factors. Brown and colleagues note systematic errors in the PAL data set, which were most apparent in the 1983–1985 and 1991–1994 time periods (Brown *pers. comm.*). These issues make monitoring of longer-term vegetation trends less reliable than those derived from the GIMMS data set. We conducted our analyses with both data sets in order to qualitatively examine the differences between them, as well as to provide results comparable with previous analyses based on the PAL data. The GIMMS-G data are available to the scientific community (e.g., through the Global Land Cover Facility, <http://glcf.umiacs.umd.edu>).

There are several advantages to using composited NDVI data sets, including the reduced effects of variable cloud cover, solar and viewing geometry, and atmospheric degradation of the surface reflectance signal (Holben, 1985; James & Kalluri, 1994; Goetz, 1997). Although the GIMMS-G data are of

improved quality over previous versions of the AVHRR record, attenuation by clouds and aerosols might not be completely ameliorated by image compositing. Kasischke and French (1997) indicated that the issue of cloud or haze contamination might still be evident in the NDVI record after image compositing. In order to minimize these effects, we scaled the NDVI values by first extracting the maximum value for each pixel in the entire NDVI time series, calculating 95% confidence interval of the maximum values for each pixel, and creating a ‘saturated’ estimate of NDVI (i.e., NDVI=1.0). NDVI values were then linearly scaled between the minimum and maximum NDVI values (i.e. NDVI/saturated value) so that any values outside the 95% limits were set to the minimum or maximum value, as appropriate. This has the effect of reducing outliers associated with sub-pixel clouds and the other residual data issues identified by Kasischke and French (1997) and others (e.g., James & Kalluri, 1994; Prince & Goward, 1995). Output NDVI for each image in the time series was then calculated as the observed NDVI value relative to the derived maximum (saturated) value, and the data sets were clipped to the extent of North America (Fig. 1). Whereas this approach does not account for spectral mixing that can occur over the 64-km<sup>2</sup> AVHRR pixels, it has the advantage of consistently scaling the observation to remove residual artifacts while permitting the original NDVI values to be backed out of the calculation, and the approach does not make assumptions of attributes associated with land cover types, canopy structure, spectral properties, shadowing, or other factors than determine NDVI in boreal forest canopies (Chen, 1996; Goetz & Prince, 1996; Huemmrich, 2001; Hyer & Goetz, 2004).

It is generally accepted that the maximum NDVI composites over the 10-day or biweekly time period represent an estimate of chlorophyll density and potential photosynthetic capacity of green vegetation. At coarse spatial scales (grain sizes) and shorter temporal scales, NDVI is most closely related to gross photosynthesis rather than net production in areas dominated by woody vegetation (e.g., forests) (Goetz & Prince, 1999; Turner et al., 2003). However, because this continues to be an area of active research, and some debate, we refer to NDVI here as simply a metric of canopy light harvesting by photosynthetically active vegetation.

##### 3.1.2. Canada large fire database

We used the Large Fire Database produced by the Canadian Fire Service (Stocks et al., 2002). The data set is a polygon coverage that contains burned area information dating from 1980 to 1997 and is the only such database of historical fires in Canada with sufficient temporal and spatial detail for consistent historical analysis (digital data are not yet released for fires after 1997). The official record of wildland fires in Canada dates back to 1918, but it is only in recent decades that the use of remotely sensed imagery has permitted consistent use of the data set (Murphy et al., 2000). Where digital information was not available, burned area polygons were hand digitized using fire management agency and Parks Canada maps. Only fires greater than 2-km<sup>2</sup> were included in the database, but these account for 97% of the total area burned (Stocks et al., 2002).

Table 1  
Summary of the PAL and GIMMS AVHRR-GAC NDVI data sets

	Period of coverage	Temporal resolution	Source
PAL	1981–1997	Pseudo10 day	<a href="http://daac.gsfc.nasa.gov/landbio/Pathfinder_Prog.shtml">http://daac.gsfc.nasa.gov/landbio/Pathfinder_Prog.shtml</a>
GIMMS	1981–2003	Biweekly	<a href="http://gimms.gsfc.nasa.gov">http://gimms.gsfc.nasa.gov</a> or <a href="http://glcf.umiacs.umd.edu/">http://glcf.umiacs.umd.edu/</a>

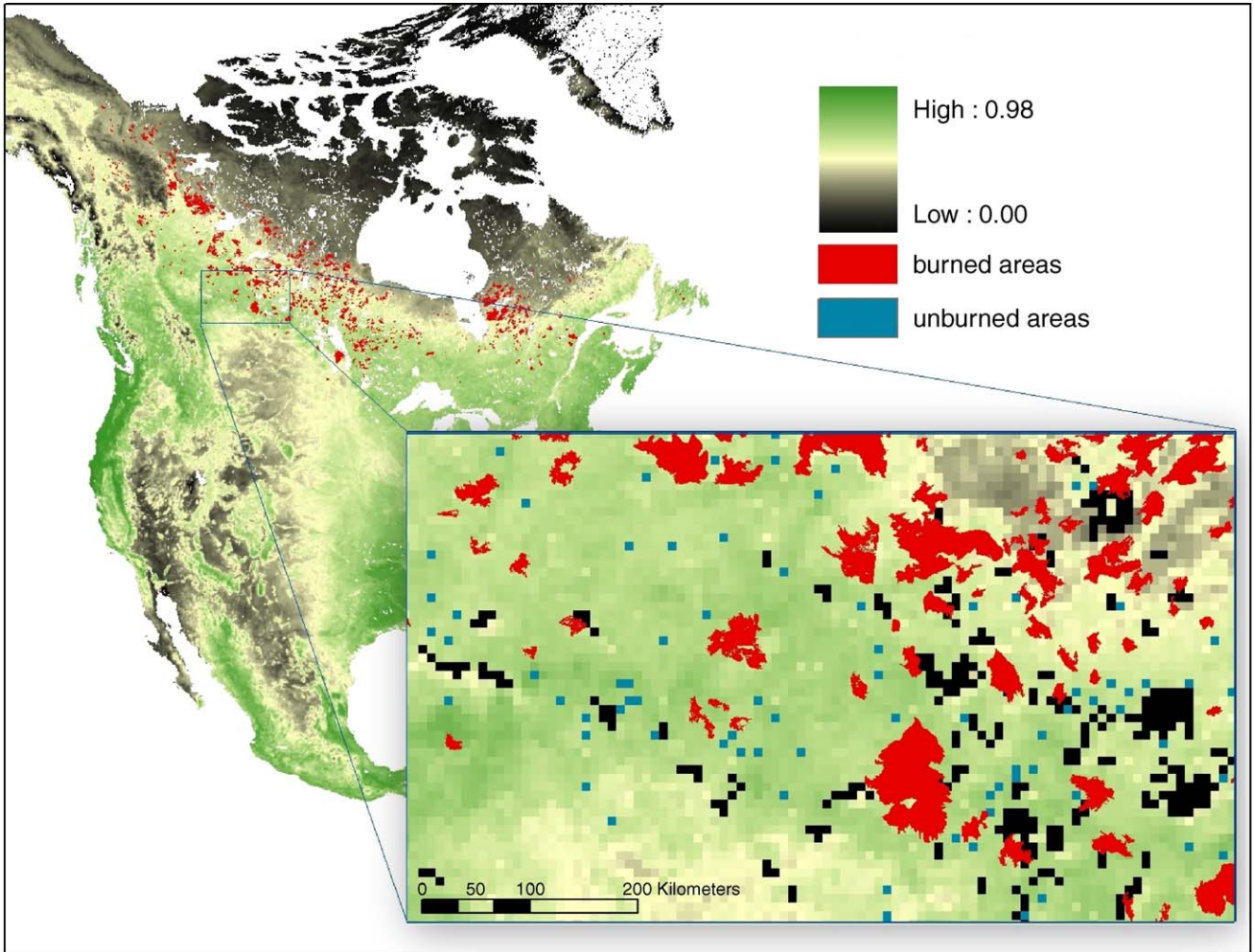


Fig. 1. An excerpt from the GIMMS AVHRR data set, showing mean NDVI at  $64\text{km}^2$  resolution for North America in the year 2000. Burned areas ( $>64\text{km}^2$ ) from the Canadian Fire Service Large Fire Database are overlaid in red. Samples of unburned areas, shown in blue, are visible in the map inset. The black pixels include water and no data.

The burned area and NDVI grids were co-registered to an Albers conic equal-area projection. The year of the fire event for each burned area polygon was translated to the attribute data, and unique coverages were created of the fire events for each year in the AVHRR time series.

### 3.1.3. Ecoregion classification

An ecoregion data set produced by the Ecological Mapping Analysis and Protocols (EcoMAP) project was acquired through the GeoGratis web site of the Natural Resource Department of Canada (<http://geogratis.cgdi.gc.ca/clf/en>). The ecoregions were defined using maps depicting climate, physiography, and existing ecological information, and each was provided a particular identification based on a prominent physiographic characteristic. Data are aggregated at four levels with the broadest level, ‘Eco-zones’, partitioning Canada into 15 generalized physiographic areas. The most detailed level, ‘Eco-districts’, stratifies 1021 areas of relatively homogeneous biophysical characteristics. We used the third level, defined by 194 ecoregions providing the detail necessary to bin burned areas into physiographic categories, while still being broad

enough to encompass the coarse  $64\text{-km}^2$  data derived from the NDVI time series.

### 3.2. Development of stratified NDVI time series

Our approach to analyzing the NDVI time series in the context of fire history and the ecoregion data sets described above is outlined in Fig. 2. For each year in the burned-area time series we subset those fires that were greater than  $64\text{km}^2$ , i.e., large enough to contain a single NDVI pixel. Furthermore, burn scars that had a circularity ratio (maximum length to width) that did not allow the coverage of an entire  $64\text{-km}^2$  grid cell were also screened and omitted. The circularity ratio allowed irregularly shaped fires, for instance, long narrow fires along drainage basins, to be omitted from the database even if the area was greater than  $64\text{km}^2$ . The remaining burned area boundaries were then converted to a gridded (raster) format with resolution comparable to the NDVI data ( $64\text{km}^2$ ). We refer to the resulting burned area masks used for sampling and extracting NDVI statistics as sampling schemes. Four sampling schemes were tested, as depicted in Fig. 3: (1) the original polygon

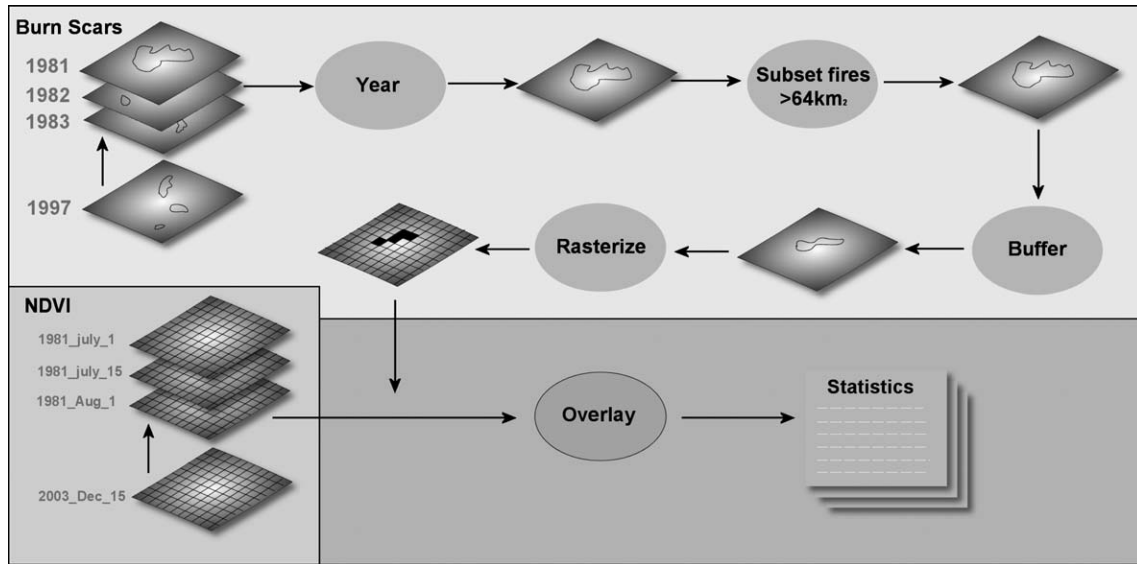


Fig. 2. Flow chart of the overall approach used to assess the AVHRR time series data sets in the context of fire history and Canadian ecoregions.

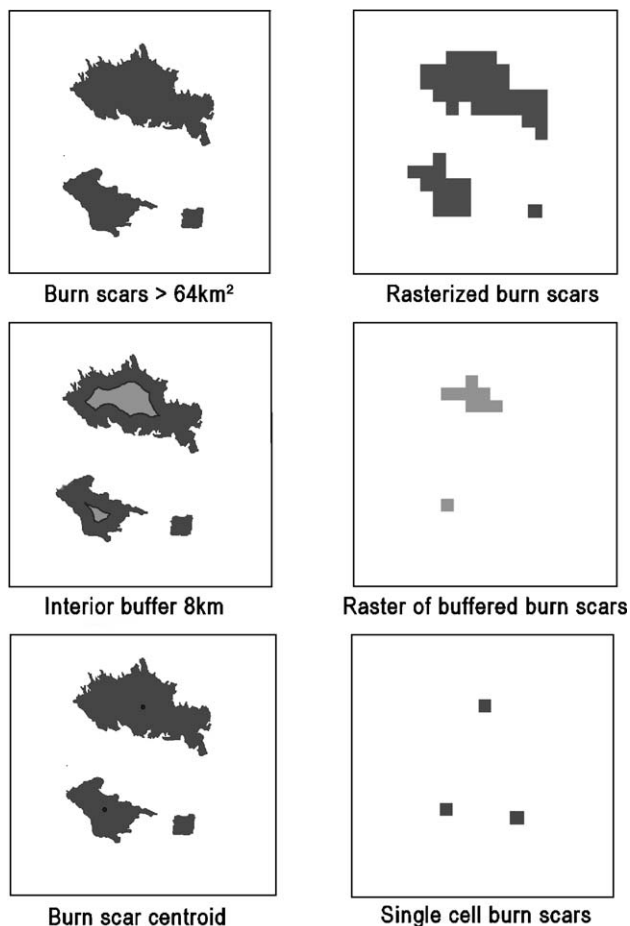


Fig. 3. Graphic representation of burned area buffering used to increase the sample size from just polygon centroids while avoiding mixed pixels at the edges of fire polygons. Line vector data were rasterized to 64 km<sup>2</sup> grid cells to match the AVHRR data. In some cases, the internal buffering caused small fires to disappear during the gridding process. In our final analysis we combined the single cell and interior buffered sampling schemes.

boundaries; (2) a buffered version of one excluding areas less than one pixel (8 km) of the burned area boundaries; (3) a single cell within each burned area boundary represented by the polygon centroid; (4) a combination of both the interior buffered and the single cell sampling schemes (although not shown in Fig. 3, this scheme is the physical union of schemes two and three).

Each scheme provided a different representation of the burned area data set to characterize the temporal characteristics of NDVI across the burned areas of Canada between 1981 and 1997. We report here only on the outcome of sampling scheme number four, which incorporates the outcome of numbers two and three, and provided the largest sample sizes (after scheme number one, which included unburned vegetation at fire boundary edges). We believe this approach best represented the variability both within and between burned areas, as discussed later. Because the boundaries of the burn scars were less well defined when represented as 8-km grid cells than in their original (polygon) format, the adopted approach provided representation of all fires greater than 64 km<sup>2</sup> but avoided errors associated with edge pixels that were a combination of burned and unburned areas. It further modified the use of a single cell (centroid or “most impacted”) to represent fires, which cannot account for the heterogeneity of regrowth within burned areas resulting from differences in fire severity, edaphic conditions, pre-burn vegetation, and so on. Finally, the buffering approach had the effect of accounting for the issue of navigation errors in the AVHRR mapping without our having to arbitrarily select a minimum window size.

Lakes and other water bodies were removed from consideration, using a surface water data set for Canada (<http://www.esri.com/data/datacd04.html>), before calculating and aggregating the NDVI statistics across the various sampling schemes. We visually inspected the effectiveness of this approach using higher resolution Landsat imagery (900 m<sup>2</sup>). We also screened the results to consider the shape of each burned area polygon so

that centroids outside of the polygon boundaries were removed from consideration.

We then developed a GIS protocol to run within the ESRI ArcGIS environment to summarize and analyze the NDVI values within the burned area boundaries for all fire years (1981–1997). This procedure ran an iterative process that selected a single fire year and calculated the mean per-pixel NDVI for all 540 15-day periods in the GIMMS 22½-year time series (July 1981 to December 2003). NDVI anomalies were expressed as departures of each of the 15-day periods from the 22½-year average. All fire years were selected consecutively and NDVI statistics were created for the time prior to fire (excluding the 1981 fires which take place at the beginning of the NDVI time series), year of fire, and recovery. A cubic smoothing spline was fit to the anomalies in order to visualize interannual trends (Chambers & Hastie, 1992). We analyzed all years but focused on three episodic fire years, 1981, 1989, and 1995, which burned large areas and spanned a range of ecoregions. NDVI time series were also created for the PAL data set, but the results reported here focus on those of the updated GIMMS-G record due to data quality issues with the PAL data, discussed later.

### 3.3. Comparison of burned and unburned area anomalies

Because the Large Fire Database does not include all fires, only the largest, selecting all areas outside of these to represent unburned areas would have incorporated smaller fires and other disturbances, complicating our attempt to isolate and compare unburned and burned areas. Instead, we created a time series of NDVI estimates for a sample of unburned areas (i.e., areas not represented in the large area fire database) by analyzing the coefficient of variation ( $CV = \text{Standard Deviation}/\text{Mean}$ ) across the entire GIMMS NDVI time series. We selected low CV areas to represent unburned areas in order to identify areas that were least likely to be influenced by land use, subpixel fires and other types of disturbance (e.g., insects), or interannual influences of climate.

A CV grid was created by stacking all the NDVI images and calculating output statistics for the entire image array, with a CV value for each grid cell. Low CV values indicated low variability in NDVI over time. A random sample of points with low CV values was selected, stratified by ecoregion, to produce a total sample of unburned area equal to the burned area of each ecoregion. The selection was weighted by using the natural breaks or Jenks' method of classification (Jenks, 1967) of the CV grid, where the lower the CV values (excluding water) were most likely to be selected. We note that this approach also consistently identified high CV areas that coincided almost entirely with fire disturbance, as identified by the burned area boundaries, confirming that these areas experienced the greatest change in NDVI over the observational period.

Large fire occurrence in Canada during the time frame of this study was mainly specific to ecoregion, i.e., fires in any given year were mostly constrained to specific ecoregions and could be adequately segregated on an ecoregion basis. For instance,

fires in 1981 occurred mostly in the Slave River lowland of Northeastern Alberta, whereas in 1989 most fires occurred in the Northwestern Quebec, central Manitoba, La Grande Hills, and Hayes River Upland ecoregions. Of the 194 ecoregions across Canada, 67 contain burn scars from fires that occurred between 1981 and 1997. We used this observation to concentrate on comparing burned and unburned areas across ecoregions in the episodic fire years (1981, 1989, and 1995), thus accounting for the regional dynamics of fire activity throughout the time series. Otherwise, the ecoregions layer was used here primarily to approximate an equal number of burned and unburned areas for each fire year.

## 4. Results and discussion

Over the 17-year record of the fire database that coincides with the AVHRR record, 1981, 1989, 1994, and 1995 experienced the highest number of fires (Fig. 4). We chose to focus on the episodic fire years 1981, 1989, and 1995 because they represent the early, middle and late portions of the time series, and each included many fires greater than  $64\text{km}^2$  (Table 2) that were relatively constrained by ecoregion. Although 1994 was similar to 1995 in terms of the number and extent of fires, the 1995 fires were constrained more tightly by ecoregion, which facilitated comparisons of burned and unburned areas.

### 4.1. Burned area assessment

Due to the spatial resolution of the AVHRR data sets, it was only possible to assess fires that burned more than  $64\text{km}^2$  (44%, 70%, 62% of all the fires in 1981, 1989, and 1995 respectively), and this selection was further reduced when the burned area edges were buffered (Fig. 4) as described earlier. There were 882 cells from all 1995 burned areas. By subtracting all the fires smaller than a single grid cell ( $64\text{km}^2$ ) the number of cells within the burned areas was reduced to 551 (62.4%). Further, after interior buffering eight km from edges the sample was reduced to just 60 cells (6.8%). In comparison, selecting a single grid cell for each 1995 fire produced 55 cells (6.2%). Thus the interior buffering process roughly doubled the burned areas sample size as compared to only sampling the centroids. This provided a good trade off between capturing the variability of the fires while limiting the amount of relatively invariant vegetation at the edges. In 1995 this amounted to a total area encompassing  $6976\text{km}^2$ . Most other years produced a comparable number of buffered cells as the simple polygon-centroid approach (Fig. 4), even though the total number of fires selected was often reduced through the buffering process. Comparable sampling for 1981 and 1989 produced 75 and 226 cells, respectively, representing areas of  $4800\text{km}^2$  and  $14,464\text{km}^2$ .

Our sampling scheme was designed to increase the number of cells that characterize the burned area, which was accomplished as noted above, and thus allowed us to better represent the spatial variability both within and between burned areas. Increasing the number of pixels in the sample incorporated a greater range of variance in the spectral characteristics of the burned vegetation cover. Visual inspection

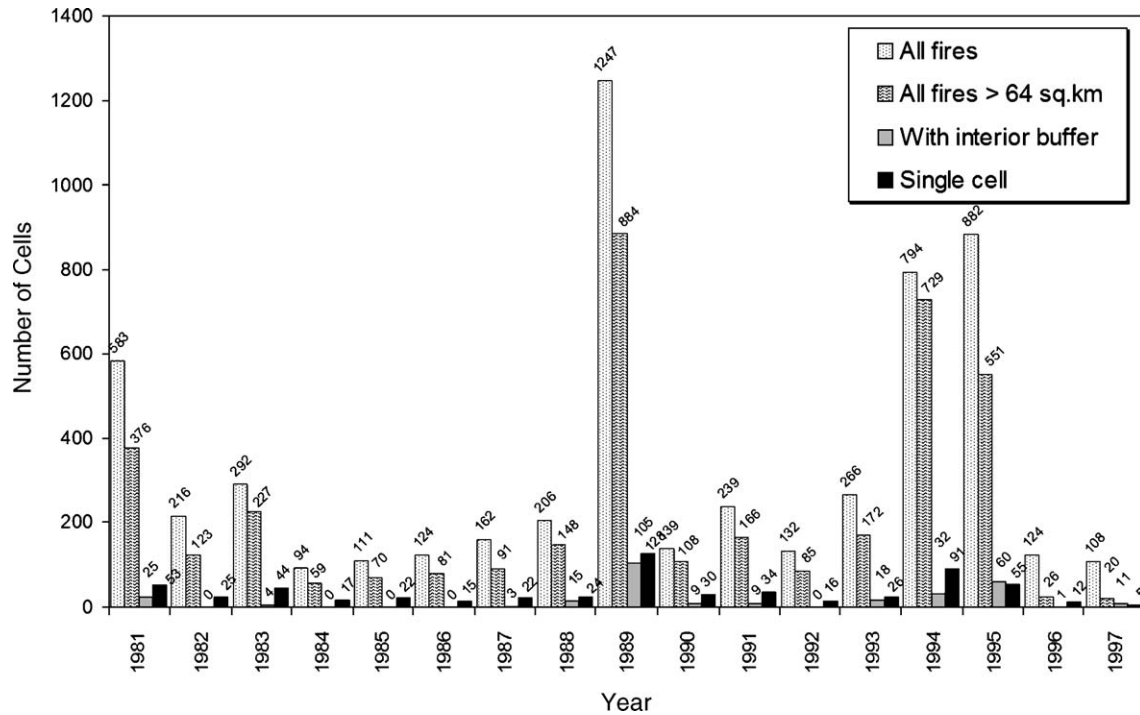


Fig. 4. The number of grid cells per sampling scheme used in aggregating the NDVI statistics in our time series. The final statistics were derived from a combination of the single cell and interior buffered sampling schemes.

of the burn coverage showed that much of the edge area in a given burn scar tended to include non-forest pixels including boundaries where fires did not spread due either to topography (e.g., ridges and coves) or land cover (e.g., marshes and barren land). We succeeded in decreasing the number of these edge areas that were substantially mixed in terms of burned and unburned vegetation, but the area within burn polygons had clearly varying degrees of burn severity, and increasing the sampling scheme as we have captured more of this variability than considering only the “most impacted” or centroid pixel within each fire. The implications of this are discussed in the following sections.

#### 4.2. Temporal variability

We stratified our selection of unburned areas by ecoregion (Fig. 5), in a similar manner to that done by Amiro et al. (2000). These areas, combined with the sample of burned areas, provided the basis for the time series of NDVI depicted in Fig. 6. The difference between the burned and unburned areas represents the response of NDVI values to disturbance over time, accounting for the influence of interannual variability in

other environmental factors captured in the unburned areas. In non-fire years, the anomaly differences represent residual variation in the NDVI signal not accounted for by ecoregion stratification, synoptic-scale climate, or disturbance. The anomaly difference showed dramatically reduced NDVI at the time of the fire for each of the three episodic fire years. The 1981 fires were characterized by a gradual period of recovery to pre-fire levels over more than a decade. Both 1989 and 1995, in contrast, displayed a sharp drop in the NDVI at the time of the fires, followed by a recovery to pre-burn levels within about five years. These recovery rates are more rapid than the typical 9-year recovery time noted by Hicke et al. (2003) in their observation of NPP trends following fire across boreal North America. The differences might be at least partly associated with our consideration of the entire suite of areas within burned areas rather than the most impacted pixel, and also our use of NDVI as a proxy for gross photosynthesis rather than NPP estimated from the NDVI and energy conversion terms (light use efficiency). Both these approaches (considering the entire burned area, and the most impacted pixel within it) might provide insight into the recovery of vegetation following fire, as well as attributes of ecological response to the intensity of disturbance and associated carbon sequestration rates. We report on differences in recovery times between ecoregions in the next section.

The comparison of the burned and unburned area anomalies for the period before the burn took place (i.e., “pre-burn”) reflects temporal variability of NDVI that is related to differences between the sites, yet unrelated to recent fire disturbance history. We analyzed the variance of the anomaly differences in data from the 1989 fire (Fig. 6b) for the seven years before the fire (1982–1989) and from 1995 to

Table 2  
Summary of fire statistics for the episodic fire years on which we focused our analysis

Year	Number of fires	Average fire size (km <sup>2</sup> )	Number of ecoregions
1981	53	454	4
1989	128	420	4
1994	91	435	7
1995	55	637	4

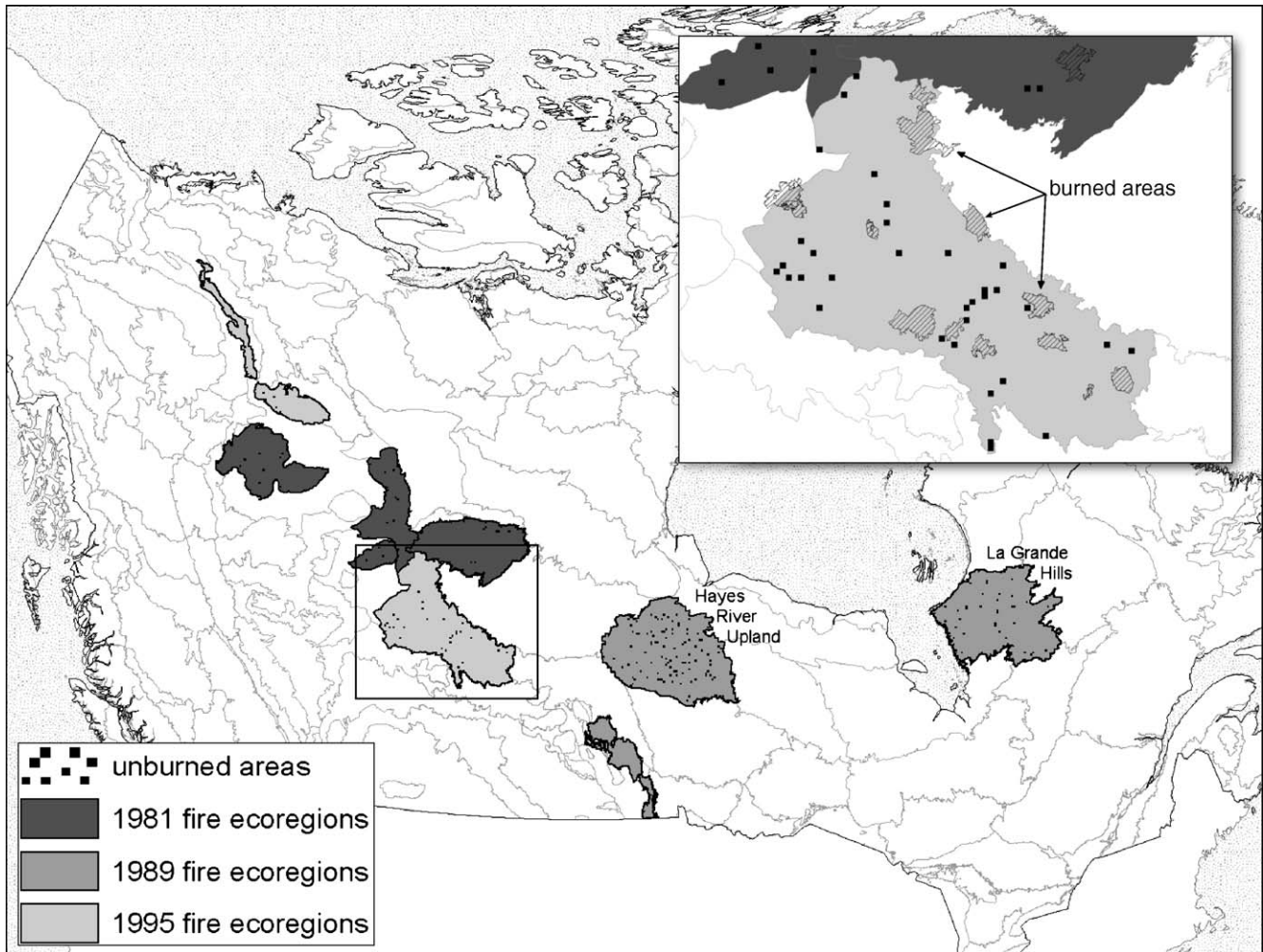
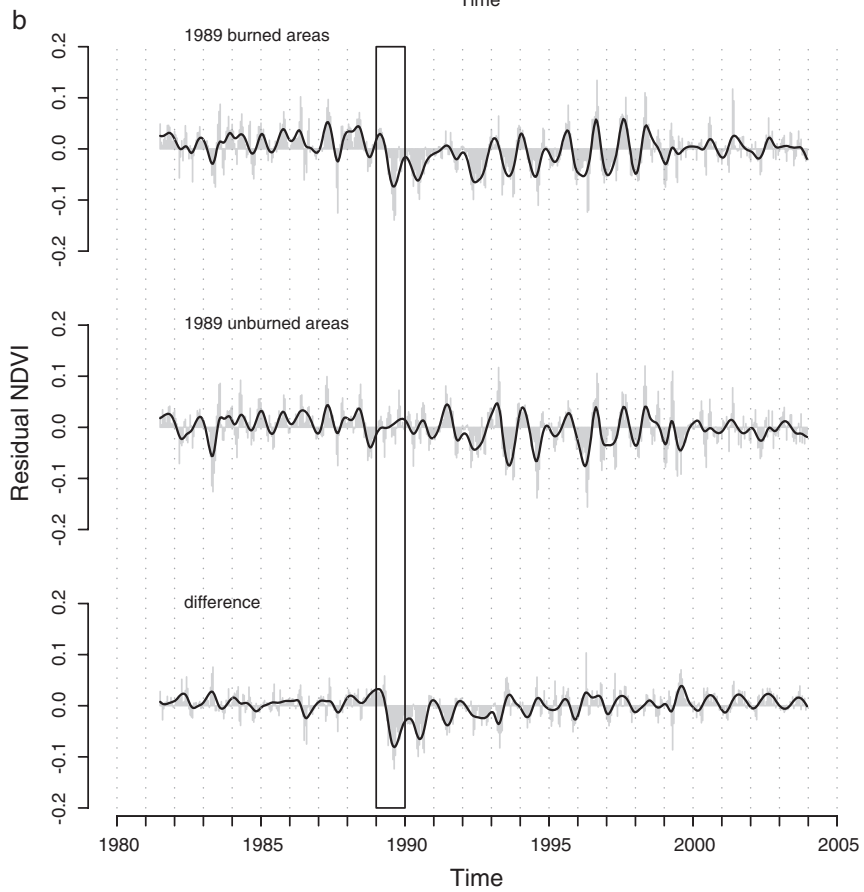
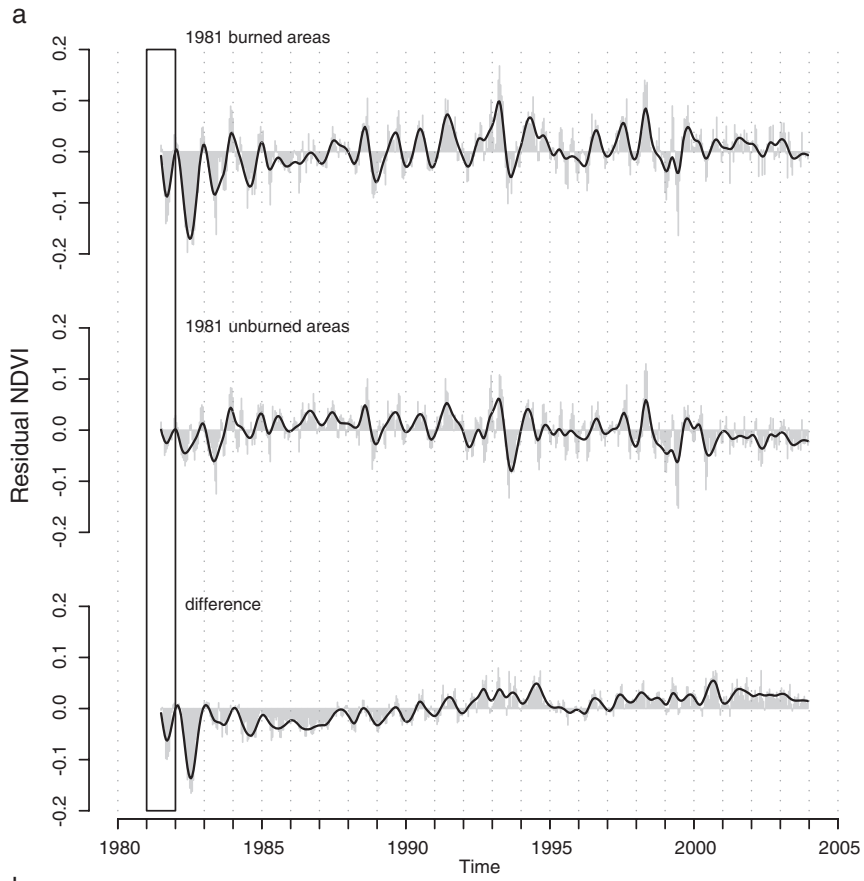


Fig. 5. Map showing 194 ecoregions across Canada and a sample of unburned areas for three episodic fire years (1981, 1989, 1995). Most fires were constrained to a few ecoregions each fire year, thus a subset of ecoregions is highlighted here. The sample of unburned areas, shown as black dots (pixels), was derived for comparison with burned areas using an equal-area coverage of burned and unburned areas per ecoregion.

2002 (allowing a five year recovery to pre-burn NDVI levels). There was very little difference in the way that pre-burn and unburned areas responded to variations in forcings other than disturbance. Following the burn, however, variance appeared to increase. We tested this by stratifying the NDVI anomalies for pre-burn and post-burn periods (i.e., subsetting 1982–1989 and 1995–2002, respectively) into seasons, and found that the variance increase occurred primarily in the early spring months (March, April, and May), with a pre-burn variance approximately double the post-burn variance ( $5.79 \times 10^{-3}$  pre-burn to  $10.74 \times 10^{-3}$ ). We performed an  $F$ -test to compare the variances and found the pre-burn and post-burn spring variance to be significantly different, rejecting null hypothesis that the true ratio of variances is equal to one ( $F=0.54$ ,  $df=41$ ,  $p$ -value=0.05). In the unburned (control) areas, pre-burn spring variance was  $2.5 \times 10^{-3}$  compared to post-burn variance of  $3.5 \times 10^{-3}$ , which was not significant under an  $F$ -test ( $F=0.40$ ,  $df=41$ ,  $p$ -value=0.27). Thus variance did not systematically change in unburned areas, but increased significantly in burned areas, and this increased variance was particularly pronounced in the spring months.

This observation of increased post-fire variability might reflect different vegetation (e.g., herbaceous and shrub versus forest) responses to temperature or precipitation variability (Xiao & Moody, 2004). The effect persisted after the recovery period, indicating that even after grasses, shrubs and saplings reestablished, they were still more likely to respond differentially to factors such as precipitation owing to, for instance, rooting depth (Kasischke & French, 1997). We were unable to make this comparison for the 1981 and 1995 burns because we lacked the appropriate time span for pre-burn and post-burn assessments. We also note that the seasonal difference in variance may support our qualitative observation that vegetation regrowth appears to be somewhat out of phase with the comparable unburned areas. In other words, burned areas appear to “green” more quickly than unburned areas, which might indicate compositional differences. A common example of this in boreal areas is deciduous regrowth (aspen and willow species) colonizing burned areas that were previously evergreen vegetation (black and white spruce), and this occurs more frequently on areas that have been more severely burned (Greene et al., 2004; Johnstone & Kasischke, 2005). We intend



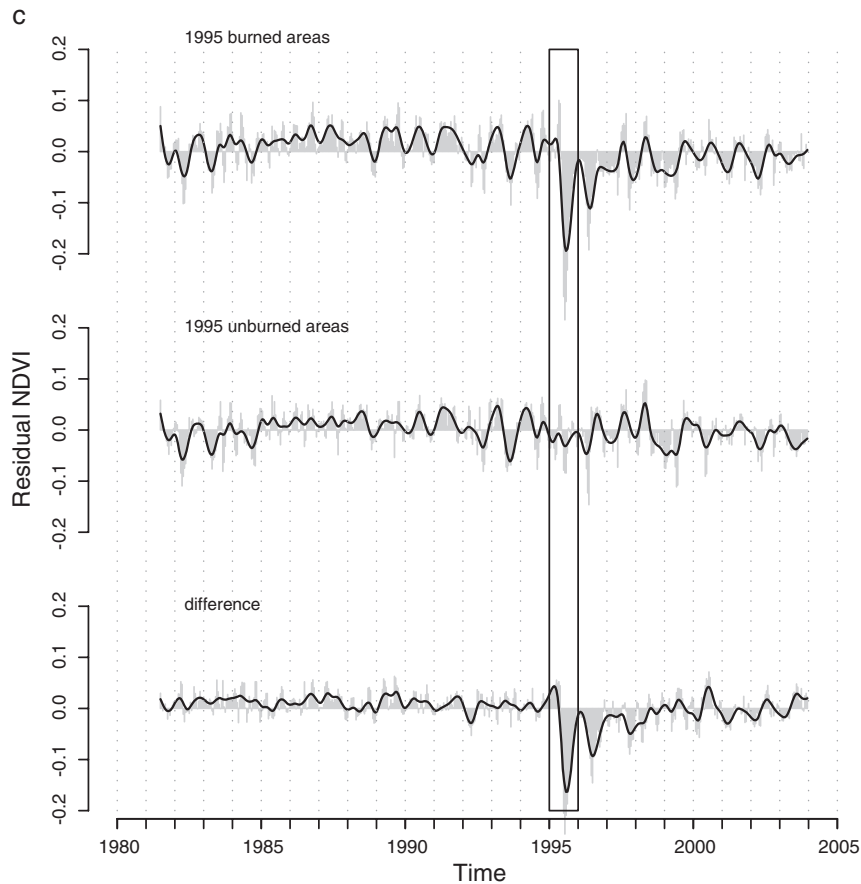


Fig. 6. NDVI anomalies (departures from full series mean) for the burned areas, unburned areas, and the difference of the two for fire years (a) 1981, (b) 1989, (c) 1995. Each was derived from the GIMMS-G data set. The solid line indicates a smoothed cubic spline fit to the data to highlight inter-annual trends.

to focus further on these observations in future work and incorporate, where possible, differences associated with spatial variability in apparent fire severity. We note here only that large within-fire variability in burn severity is common across burned area of boreal forest, and that we attempted to capture this variability by incorporating as large a sample size as possible, subject to the constraints described in Section 3.1.

#### 4.3. Local to regional scale variability

The location of the majority of the fires in 1995 were in ecoregions within close proximity to the 1981 fires (the upper Canadian Rockies, northern Alberta, Saskatchewan, and Northwest Territories), but the 1989 fires were more widespread and covered different types of ecoregions (southern and central Manitoba and western Quebec Provinces). This might be related to differences in fire conditions and severity between years, as well as differences in fire regimes between ecoregions. Comparison of two distinct ecoregions with a large number of fires in 1989, one dominated by conifer forest (Hayes river upland) and one with equal components of conifer and transitional forest (i.e., less than 10% forest cover) (La Grande Hills), indicated a similar recovery period following disturbance (Fig. 7). Hicke

et al. (2003) noted differences between ecoregions in NPP recovery following fire, which one might expect between vegetation types and their response to disturbance. Amiro et al. (2000) also noted ecoregion differences in NPP following fire, particularly between forest and tundra dominated ecoregions. These observations are also consistent with recent differences in growth trends noted across boreal North American (Bunn et al., 2005; Goetz et al., 2005). Nonetheless, while the magnitude of NPP differs between ecoregions, even

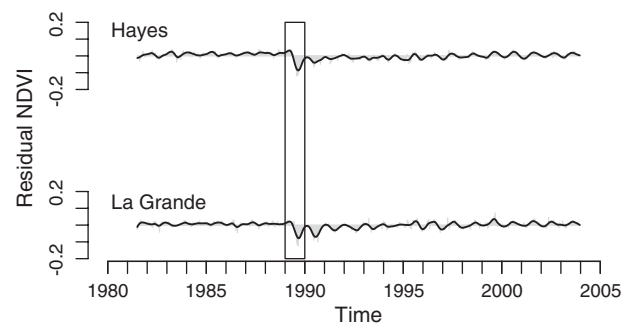


Fig. 7. Difference of the NDVI anomalies and unburned area anomalies for the Hayes River Upland and the LaGrande Hills ecoregions in Canada. Both ecoregions had a high number of fires during 1989.

Table 3  
Rank correlation between coefficients of variation in the anomalies of GIMMS NDVI for areas within the buffered burned area boundaries, for each of three episodic fire years

Year	Average low CV	Average high CV	Correlation coefficient	Sample size
1981	0.53	0.69	0.73	53
1989	0.62	0.72	0.94	105
1995	0.52	0.63	0.88	58

Low CV values are associated with less severely burned areas, whereas high-CV values are indicative of more severe burning (i.e., most impacted). Areas burned are as indicated in Table 2. All correlation coefficients were significant at the  $p < 0.0001$  level.

in their recovery following disturbance, our results indicate that the time for vegetation cover to reestablish was similar between the ecoregions on which we focused. This similarity may be a result of the early colonization of fire-disturbed areas by grasses and other herbaceous vegetation types, which are then gradually replaced by woody plants (Amiro et al., 2000; Johnstone et al., 2004; Zimov et al., 1999).

Because the fire database includes only large fires, variability within fires can be as great as between them. To examine this more closely we visually inspected Landsat Thematic Mapper imagery for some of the burned areas. These revealed that not all of the fires were contained within forested areas, but crossed into grassland, peat bogs, and fens. Assuming that these land-cover types burn at different levels of severity associated with surface conditions and fuel loads, and also that they recover differently from fire disturbance, the NDVI anomalies and recovery times reflect the whole ecosystem response to the heterogeneity of fire behavior. Further, interannual variations in vegetation activity associated with climate could influence regrowth rates and patterns (Bunn et al., 2005). For example, a cold wet spring in a year following a fire might reduce the NDVI values in the burned and unburned anomalies. It is important to consider these issues of climatic variability, as well as associated spatial variability in fire severity, when interpreting vegetation recovery rates and patterns.

Further indication of this within-fire versus between-fire variability was provided by a comparison using growing season values for each 15-day AVHRR interval for all fires in 1995, where we averaged all pixels within buffered burned areas and also averaged values for each burned area first and then averaged across all fires. The comparison indicated that either method (averaging all burned area pixels or averaging across burned areas) produced essentially the same result ( $R^2 = 0.99$ , slope = 0.90, standard error = 0.012,  $p < 0.0001$ ). The derived NDVI values ranged the full spectrum between 0.2 and 0.8, averaging  $\sim 0.58$ . Similar results were noted for the 1989 burns ( $R^2 = 0.99$ , slope = 0.93, standard error = 0.01, mean = 0.41,  $p < 0.0001$ ). This result indicates that our sampling scheme of incorporating all eligible pixels across all burned areas was not significantly different than first averaging the values within and then across all fires (e.g., 1995 fires), as well as confirming that within and between fire variability was comparable across the region. The most robust test of this was the 1989 fires, which were characterized by one very large fire in northern

Manitoba and many smaller fires more evenly distributed across the region.

Finally, we compared coefficients of variation in the time-series anomalies for each pixel within each buffered fire boundary, in order to focus more closely on within-fire variability associated with burn severity. We estimated this with the same approach used to select unburned areas, i.e. areas with low CV values through the time series, and compared these with high CV pixels (areas likely to have burned more severely). The results indicate that there was substantially different information captured when considering all pixels within a fire versus only those most impacted by fire (Table 3). Correlation coefficients between the anomaly CV values ranged from 0.73 in 1981 to 0.94 in 1989, indicating that within-fire severity was less heterogeneous in 1989 than in the other episodic fire years. We note that all of the derived CV values within fire boundaries were substantially higher than the comparisons with unburned areas, as expected for areas that experienced some degree of burning, and they indicate that within-fire variability in the CV values was associated with differences in burn severity.

#### 4.4. Comparison of the GIMMS and PAL data sets

The two AVHRR data sets yielded different results in NDVI dynamics over time within the burned area boundaries. Analysis of the departure from the mean (anomalies) showed a sharp decline in mean NDVI for both the PAL and GIMMS data sets in the 1981 and 1995 burned areas (not shown), but in 1989 there was only a slightly negative NDVI anomaly in the PAL data whereas the GIMMS record captured a large negative anomaly (Fig. 8).

The PAL data systematically estimated higher NDVI than the GIMMS data set, and this carried through to the calculation of NDVI (Fig. 9). Because the PAL data set was produced as 10-day composites, and the GIMMS was biweekly, comparisons of results was based on differences smoothing splines fit to the two time series (Fig. 8). There were substantial differences between the NDVI time series derived from the two data sets, with the GIMMS data more clearly capturing the reduction in NDVI associated with disturbance events. If the GIMMS data more

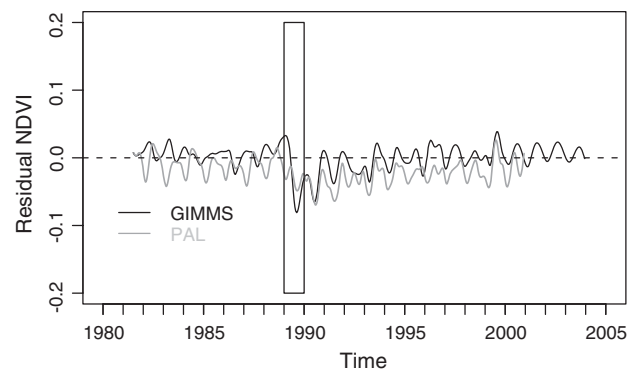


Fig. 8. Difference of the burned and unburned area NDVI anomalies for 1989, derived from both the GIMMS-G and the PAL data sets. The GIMMS data set more clearly captures the fire disturbance and recovery trajectory.

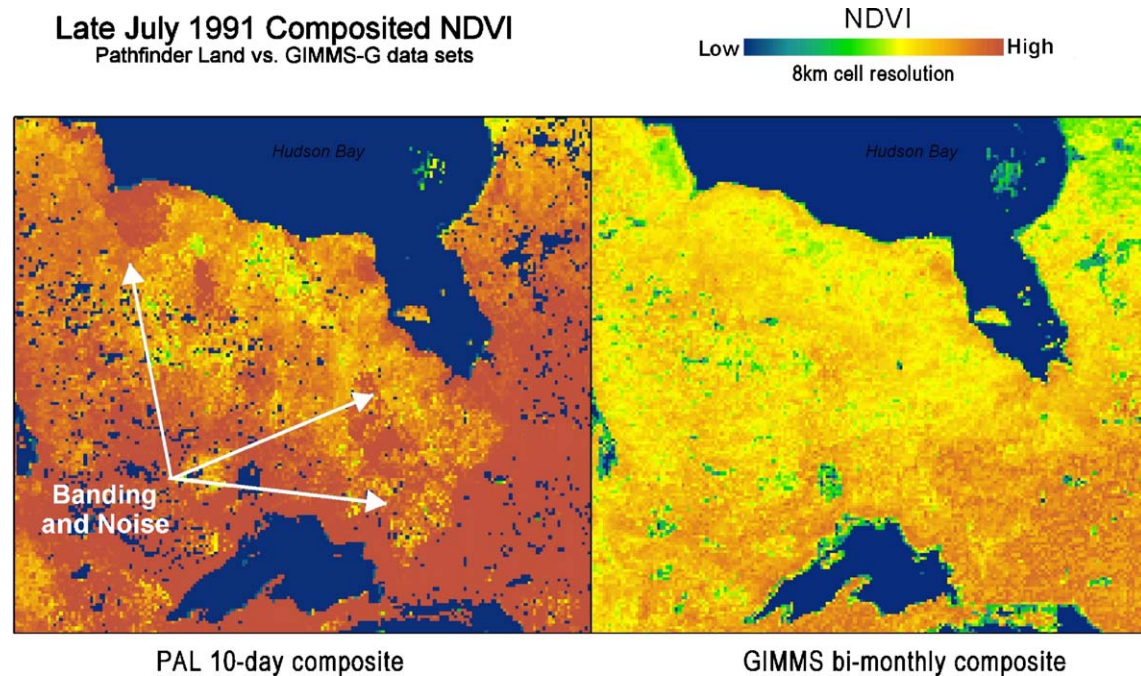


Fig. 9. Comparison of the Pathfinder Land NDVI and the GIMMS-G NDVI data sets. Both images are the same date and location, late July, 1991. Significant banding, 'noisy' areas, and systematic over estimation of NDVI values are common among the Pathfinder data.

accurately characterized the reduction in NDVI at the time of the fire, it is logical to assume that it is also capturing the recovery trajectories that followed.

Discrepancies between the two data sets were apparent when the time series data were animated as a video sequence. Some years in the PAL data set displayed large areas of noise (nearly random data values), as well as 'banding' associated with orbital paths (Fig. 9). The GIMMS data set had fewer 'no data' pixels, which were abundant in the PAL data. These artifacts in the PAL data were most evident in Alaska and Northwest Canada, yet were also noticeable in parts of Quebec and the Canadian Rockies. The noise problem was particularly evident in the later portion of the growing season. Similar observations were noted and quantified by Brown et al. (pers. comm.), but a more detailed assessment of differences between the data sets is beyond the scope of the current study. It would require interpolating the 10-day PAL to the 15-day GIMMS time step, or otherwise recomputing the composited data to a common time interval. It might also require deconvolving or reproducing the various corrections made to each time series data set. Users of the PAL data set should be aware of these issues, which influence its merits relative to more recent modifications inherent in the GIMMS-G data set.

Related work monitoring fire disturbance in boreal forest vegetation suggests that spectral vegetation indices derived from SPOT VGT data better reveal the complexity of vegetation regeneration patterns following fire, owing to better geometric fidelity and spectral properties (Fraser & Li, 2002; Mollicone et al., 2002). These data sets take longer to saturate following fire, and are sensitive to strong visible light absorption by the char combustion products of fire before regeneration occurs. We note

some potential evidence for this in Fig. 6, just before the vegetation regrowth ensues. A fuller analysis of these observations might include assessments with finer spectral resolution imagery, and stratifying the vegetation types within each ecoregion, perhaps with higher spatial resolution imagery or land cover data, and comparing recovery times between vegetation types.

## 5. Conclusion

The AVHRR time-series data sets used in this study provide metrics of canopy light harvesting and photosynthetic activity over the past two decades across large areas. Our goal was to examine two interpretations of the AVHRR NDVI time-series, the Pathfinder-Land (PAL) and the GIMMS-G data sets (64 km<sup>2</sup>), in the context of large fire disturbances in the boreal forest ecosystems of Canada. We have shown the efficacy of using these data sets to track depletion and regrowth of vegetation, and to assess spatial and temporal variability changes both before and following fire disturbance. Although all of the fires were spatially heterogeneous, enhanced sampling of burned areas using a buffering and filtering scheme allowed us to focus analysis on only those fires which met criteria than minimized mixed pixels at the edges of identified burned areas. This, in turn, allowed us to make use of both the GIMMS and PAL data sets for evaluating the impact of the fire disturbance on NDVI through time.

We analyzed all fire years from 1981 through 1997 but focused our analysis on three episodic fire years — 1981, 1989, and 1995. All three years showed a significant departure from the series mean NDVI values at the time of fire disturbance. By coupling this information with similar statistics aggregated from

unburned areas in the same ecoregions for each fire year, we were able to account for variations in the mean NDVI value over time that resulted from factors other than fire disturbance. Our results indicated that fire disturbance was distinct when compared with unburned areas, and that accounting for the temporal variability of NDVI within unburned areas aided the definition of recovery times to pre-burn levels, which typically took five years or more following fire. These results support earlier work (Amiro et al., 2000; Chen et al., 2003; Hicke et al., 2003), but the observed recovery rates were shorter than previously noted. This observation is likely due to our accounting for spatial variability within burned areas rather than focusing on the most impacted areas. Both of these approaches (i.e., all areas of varying burn severity, and only the most impacted) provide insight into the recovery of vegetation following different intensities of fire disturbance.

Our results also indicated changes in NDVI pre-burn versus post-burn, the latter following recovery to pre-burn levels, which we suggest are associated with vegetation compositional changes following fire. This finding is consistent with the establishment of pioneer species dominated primarily by herbaceous vegetation and sparse woody shrubs and saplings. Finally, the results emphasize the utility of the reprocessed and newly released GIMMS-G data set (Brown et al., 2004), which better characterized the impact of fire disturbance and recovery of canopy NDVI that followed, while permitting refined comparisons of changes in burned versus unburned areas, and pre- versus post-burn variability through time.

Continent-wide monitoring of vegetation response to fire over time can be an effective ingredient for climate and carbon system models (Bunn et al., 2005; Goetz et al., 2005). The characteristics of forest canopy recovery from fire and its influence on carbon sequestration are rich avenues for future research, particularly in fire-dominated systems such as the boreal biome. This work will be used as a baseline for time series analysis of boreal vegetation dynamics across North America, incorporating data sets derived from the MODIS (Moderate Resolution Imaging Spectroradiometer) and NPOESS (National Polar-Orbiting Operational Environmental Satellite System) satellites into a consistent monitoring system.

## Acknowledgements

We would like to thank the anonymous referees whose careful reviews resulted in a more meaningful analysis and a much improved manuscript. We also acknowledge invaluable input from Eric Kasischke, as well as Jim Tucker and Brian Stocks for their data sets. This work was funded by the NOAA Carbon Cycle Science program, and by earlier support from the NASA ADRO program.

## References

Angert, A., Biraud, S., Bonfils, C., Henning, C. C., Buermann, W., Pinzon, J., et al. (2005). Drier summers cancel out the CO<sub>2</sub> uptake enhancement induced by warmer springs. *Proceedings of the National Academy of Sciences*, 102, 10823–10827.

- Amiro, B. D., Chen, J. M., & Liu, J. (2000). Net primary productivity following forest fire for Canadian ecoregions. *Canadian Journal of Forest Research*, 30(6), 939–947.
- Amiro, B. D., MacPherson, I. J., Desjardins, R. L., Chen, J. M., & Liu, J. (2003). Post-fire carbon dioxide fluxes in the western Canadian boreal forest: Evidence from towers, aircraft and remote sensing. *Agricultural and Forest Meteorology*, 115, 91–107.
- Bailey, R. G. (1998). *Ecoregions: The ecosystem geography of the oceans and continents*. New York, NY, USA: Springer-Verlag, (176 pp).
- Baldocchi, D., Falge, E., Gu, L. H., Olson, R., Hollinger, D., Running, S., et al. (2001). FLUXNET: A new tool to study the temporal and spatial variability of ecosystem-scale carbon dioxide, water vapor, and energy flux densities. *Bulletin of the American Meteorological Society*, 82, 2415–2434.
- Bonan, G. B., Chapin, F. S., & Thompson, S. L. (1995). Boreal forest and tundra ecosystems as components of the climate system. *Climate Change*, 29, 145–167.
- Bousquet, P., Peylin, P., Ciais, P., Le Quere, C., Friedlingstein, P., & Tans, P. P. (2000). Regional changes in carbon dioxide fluxes of land and oceans since 1980. *Science*, 290, 1342–1346.
- Brown, M. E., Pinzon, J. E., & Tucker, C. J. (2004). New vegetation index data set to monitor global change. *American Geophysical Union EOS Transactions*, 85(52), 565–569.
- Bunn, A. G., Goetz, S. J., & Fiske, G. J. (2005). Observed and predicted responses of plant growth to climate across Canada. *Geophysical Research Letters*, 32, L16710.
- Chambers, J. M., & Hastie, T. J. (1992). *Statistical models in S*: Wadsworth and Brooks/Cole.
- Chen, J. (1996). Canopy architecture and remote sensing of the fraction of photosynthetically active radiation absorbed by boreal forest conifers. *IEEE Transactions on Geoscience and Remote Sensing*, 34, 1353–1368.
- Chen, J. M., Ju, W., Cihlar, J., Price, D., Liu, J., Chen, W., et al. (2003). Spatial distribution of carbon sources and sinks in Canada's forests based on remote sensing. *Tellus B*, 55, 622–642.
- Cubasch, U., Meehl, G.A., Boer, G.J., et al. (2001). Projections of Future Climate Change. Chapter 9 in Houghton, J.T., Ding, Y., Griggs, D.J., et al., editors. *Climate Change 2001: The Scientific Basis*. Contributions of Working Group I to the Third Assessment Report of the IPCC. Cambridge University Press, Cambridge, UK.
- Easterling, D. R., Karl, T. R., Gallo, K. P., Robinson, D. A., Trenberth, K. E., & Dai, A. (2000). Observed climate variability and change of relevance to the biosphere. *Journal of Geophysical Research*, 105(D15), 20101–20114.
- Folland, C.K., Karl, T.R., Christy, J.R., Clarke, R.A., Gruba, G.V., Jouzel, J., et al. (2001). Chapter 2. Observed Climate Variability and Change. In: *Climate Change 2001: The Scientific Basis*. Contribution of Working Group I to the Third Assessment Report of the Intergovernmental Panel on Climate Change. (p. 181) Cambridge University Press.
- Fraser, R. H., & Li, Z. (2002). Estimated fire-related parameters in boreal forest using SPOT VEGETATION. *Remote Sensing of Environment*, 82, 95–110.
- Goetz, S. J. (1997). Multi-sensor analysis of NDVI, surface temperature, and biophysical variables at a mixed grassland site. *International Journal of Remote Sensing*, 18, 71–94.
- Goetz, S. J., Bunn, A. G., Fiske, G. J., & Houghton, R. A. (2005). Satellite observed photosynthetic trends across boreal North America associated with climate and fire disturbance. *Proceedings of the National Academy of Sciences*, 103(38), 13521–13525.
- Goetz, S. J., & Prince, S. D. (1996). Remote sensing of net primary production in boreal forest stands. *Agricultural and Forest Meteorology*, 78, 149–179.
- Goetz, S. J., & Prince, S. D. (1999). Modeling terrestrial carbon exchange and storage: Evidence and implications of functional convergence in light use efficiency. *Advances in Ecological Research*, 28, 57–92.
- Goulden, M. L., Wofsy, S. C., Harden, J. W., Trumbore, S. E., Crill, P. M., Gower, S. T., et al. (1998). Sensitivity of boreal forest carbon balance to soil thaw. *Science*, 279, 214–216.
- Greene, D. F., Noel, J., Bergeron, Y., Rousseau, M., & Gauthier, S. (2004). Recruitment of *Picea mariana*, *Pinus banksiana*, and *Populus tremuloides* across a burn severity gradient following wildfire in the southern boreal forest of Quebec. *Canadian Journal of Forest Research*, 34(9), 1845–1857.

- Griffis, T. J., Black, T. A., Morgenstern, K., Barr, A. G., Nestic, Z., Drewitt, G. B., et al. (2003). Ecophysiological controls on the carbon balances of three southern boreal forests. *Agricultural and Forest Meteorology*, *117*, 53–71.
- Hall, F. G. (1999). BOREAS in 1999: Experiment and science overview. *Journal of Geophysical Research*, *104*(D22), 27,627–27,639.
- Harden, J. W., Trumbore, S. E., Stocks, B. J., Hirsch, A., O'Neill, K. P., & Kasischke, E. S. (2000). The role of fire in the boreal carbon budget. *Global Change Biology*, *6*(Suppl. 1), 174–184.
- Hicke, J. A., Asner, G. P., Kasischke, E. S., French, N. H. F., Randerson, J. T., Collatz, G. J., et al. (2003). Postfire response of North American boreal forest net primary productivity analyzed with satellite observations. *Global Change Biology*, *9*(8), 1145–1157.
- Holben, B. (1985). Characteristics of maximum-value composite images from temporal AVHRR data. *International Journal of Remote Sensing*, *7*, 1417–1434.
- Houghton, R. A. (2003). Why are estimates of the terrestrial carbon balance so different? *Global Change Biology*, *6*, 500–535.
- Huemrich, K. F. (2001). The GeoSail Model: A simple addition to the SAIL Model to describe discontinuous canopy reflectance. *Remote Sensing of Environment*, *75*, 423–431.
- Hyer, E., & Goetz, S. J. (2004). Comparison and sensitivity analysis of instruments and radiometric methods for LAI estimation: Assessments from a boreal forest site. *Agricultural and Forest Meteorology*, *122*, 157–174.
- James, M. E., & Kalluri, S. N. V. (1994). The Pathfinder AVHRR land data set: An improved coarse resolution data set for terrestrial monitoring. *International Journal of Remote Sensing*, *15*, 17.
- Jenks, G. F. (1967). The data model concept in statistical mapping. *International Yearbook of Cartography*, *7*, 186–190.
- Johnstone, J. F., Chapin, I. F. S., Foote, J., Kemmett, S., Price, K., & Viereck, L. (2004). Decadal observations of tree regeneration following fire in boreal forests. *Canadian Journal of Forest Research*, *34*(2), 267–273.
- Johnstone, J. F., & Kasischke, E. S. (2005). Stand-level effects of soil burn severity on postfire regeneration in a recently burned black spruce forest. *Canadian Journal of Forest Research*, *38*, 2151–2163.
- Kasischke, E. S., & French, N. H. F. (1997). Constraints on using AVHRR composite index imagery to study patterns of vegetation cover in boreal forests. *International Journal of Remote Sensing*, *18*(11), 2403–2426.
- Kasischke, E. S., & Stocks, B. J. (Eds.). (2000). *Fire, climate change and carbon cycling in the boreal forest. Ecological Studies Series, Vol. 138*. (pp. 461274–288) New York: Springer.
- Keeling, C. D., Chin, J. F. S., & Whorf, T. P. (1996). Increased activity of northern vegetation inferred from atmospheric CO<sub>2</sub> measurements. *Nature*, *382*, 146–149.
- Kurz, W. A., & Apps, M. J. (1999). A 70-year retrospective analysis of carbon fluxes in the Canadian forest sector. *Ecological Applications*, *9*(2), 526–547.
- Liu, H. P., Randerson, J. T., Lindfors, J., & Chapin, F. S. (2005). Changes in the surface energy budget following fire in boreal ecosystems of interior Alaska: An annual perspective. *Journal of Geophysical Research-Atmospheres*, *110*, doi 10.1029/2004JD005158
- Lucht, W., Prentice, I. C., Myneni, R. B., Sitch, S., Friedlingstein, P., et al. (2002). Climatic control of the high-latitude vegetation greening trend and Pinatubo effect. *Science*, *296*, 1687–1689.
- McGuire, A. D., Sitch, S., & Wittenberg, U. (2001). Carbon balance of the terrestrial biosphere in the twentieth century: Analyses of CO<sub>2</sub>, climate, and land use effects with four process-based ecosystem models. *Global Biogeochemical Cycles*, *15*, 183.
- Mollicone, D., Achard, F., Marchesini, L. B., Federici, S., Wirth, C., Leipold, M., et al. (2002). A remote sensing based approach to determine forest fire cycle: Case study of the Yenisei Ridge dark taiga. *Tellus*, *54*(5), 688–695.
- Murphy, P. J., Mudd, J. P., Stocks, B. J., Kasischke, E. S., Barry, D., Alexander, M. E., et al. (2000). Historical fire records in the North American boreal forest. In E. S. Kasischke, & B. J. Stocks (Eds.), *Fire, climate change and carbon cycling in the Boreal Forest Ecological Studies Series*. (pp. 274–288) New York: Springer-Verlag.
- Myneni, R. B., Keeling, C. D., Tucker, C. J., Asrar, G., & Nemani, R. R. (1997). Increased plant growth in the northern high latitudes for 1981 to 1991. *Nature*, *386*, 698–702.
- Nemani, R. R., Keeling, C. D., Hashimoto, H., Jolly, W. M., Piper, S. C., Tucker, C. J., et al. (2003). Climate-driven increases in global terrestrial net primary production from 1982 to 1999. *Science* (5625), 1560–1562.
- Pinzon, J., Brown, M. E., & Tucker, C. J. (2004). Satellite time series correction of orbital drift artifacts using empirical mode decomposition. In Hilbert-Huang Transform: *Introduction and Applications*, eds. N. Huang, pp. Chapter 10, Part II.
- Prince, S. D., & Goward, S. J. (1995). Global primary production: A remote sensing approach. *Journal of Biogeography*, *22*, 815–835.
- Randerson, J. T., Field, C. B., Fung, I. Y., & Tans, P. P. (1999). Increases in early season net ecosystem uptake explain changes in the seasonal cycle of atmospheric CO<sub>2</sub> at high northern latitudes. *Geophysical Research Letters*, *26*, 2765–2768.
- Slayback, D. A., Pinzon, J. E., Los, S. O., & Tucker, C. J. (2003). Northern hemisphere photosynthetic trends 1982–99. *Global Change Biology*, *9*, 1–15.
- Stocks, B. J., Fosberg, M. A., Wotton, M. B., Lynham, T. J., & Ryan, K. C. (2000). Climate change and forest fire activity in North American boreal forests. In E. S. Kasischke, & B. J. Stocks (Eds.), *Fire, climate change and carbon cycling in the Boreal forest* (pp. 368–376). Inc., New York: Springer-Verlag.
- Stocks, B. J., Mason, J. A., Todd, J. B., Bosch, E. M., Wotton, B. M., Amiro, B. D., et al. (2002). Large forest fires in Canada, 1959–1997. *Journal of Geophysical Research*, *107*.
- Tucker, C. J., Pinzon, J. E., Brown, M. E., Slayback, D., Pak, E. W., Mahoney, R., et al. (2005). An Extended AVHRR 8-km NDVI Data Set Compatible with MODIS and SPOT Vegetation NDVI Data. *International Journal of Remote Sensing*, *26*(20), 4485–4498.
- Turner, D. P., Urbanski, S., Bremer, D., Wofsy, S. C., Meyers, T., Gower, S. T., et al. (2003). A cross-biome comparison of daily light use efficiency for gross primary production. *Global Change Biology*, *9*, 383–395.
- Walsh, J. E., Kattsov, V. M., Chapman, W. L., Govorkova, V., & Pavlova, T. (2002). Comparison of Arctic climate simulations by uncoupled and coupled global models. *Journal of Climate*, *15*(12), 1429–1446.
- Xiao, J., & Moody, A. (2004). Photosynthetic activity of US biomes: Responses to the spatial variability and seasonality of precipitation and temperature. *Global Change Biology*, *10*(4), 437–451.
- Zimov, S. A., Davidov, S. P., Zimova, G. M., Davidova, A. I., Chapin III, F. S., Chapin, M. C., et al. (1999). Contribution of disturbance to increasing seasonal amplitude of atmospheric CO<sub>2</sub>. *Science*, *284*, 1973–1976.